

AWH/IPNS/CP -
CONF-9707128--

93965

**Neutron Scattering Characterization of Microstructure in Uranium Silicides,
Ceramic Composites and Ni-Based Alloys**

J. W. Richardson, Jr

*Intense Pulsed Neutron Source (IPNS) Division
Argonne National Laboratory
Argonne, IL 60439 USA*

RECEIVED
NOV 04 1997
OSTI

The submitted manuscript has been authored by a contractor of the U. S. Government under contract W-31-109-ENG-38. Accordingly, the U. S. Government retains a nonexclusive, royalty-free license to publish or reproduce the published form of this contribution, or allow others to do so, for U. S. Government purposes.

DISTRIBUTION OF THIS DOCUMENT IS UNLIMITED



MASTER

To be published in Conference Proceedings:

“Computer Aided Design of High Temperature Materials”

eds., A. Pechenik, R. K. Kalia and P. Vashishta

Oxford University Press

*Work supported by U. S. Department of Energy, BES, contract No. W-31-109-ENG-38

DISCLAIMER

This report was prepared as an account of work sponsored by an agency of the United States Government. Neither the United States Government nor any agency thereof, nor any of their employees, makes any warranty, express or implied, or assumes any legal liability or responsibility for the accuracy, completeness, or usefulness of any information, apparatus, product, or process disclosed, or represents that its use would not infringe privately owned rights. Reference herein to any specific commercial product, process, or service by trade name, trademark, manufacturer, or otherwise does not necessarily constitute or imply its endorsement, recommendation, or favoring by the United States Government or any agency thereof. The views and opinions of authors expressed herein do not necessarily state or reflect those of the United States Government or any agency thereof.

DISCLAIMER

**Portions of this document may be illegible
in electronic image products. Images are
produced from the best available original
document.**

NEUTRON SCATTERING CHARACTERIZATION OF MICROSTRUCTURE IN URANIUM SILICIDES, CERAMIC COMPOSITES AND Ni-BASED ALLOYS

JAMES W. RICHARDSON, JR.

Intense Pulsed Neutron Source Division

Argonne National Laboratory

Argonne, IL 60439, U.S.A.

1. Introduction

Neutron scattering has proven to be a valuable tool for studying the microstructural properties of technologically important materials. The exceptionally high penetration power of neutrons enables the investigation of bulk materials, while unusual scattering contrasts observed in many materials provide unique access to important properties. Macroscopic performance of components under extreme conditions, which ultimately determines their viability for special applications, is often closely related to microstructural properties such as particle size, residual stress and phase stability. Neutron scattering experiments performed with samples exposed to realistic environmental conditions provide direct correlations between microscopic and macroscopic properties. Neutron irradiation of uranium silicide (a prospective reactor fuel), is used here as a prototypical example of *in situ* residual stress generation and evolution, accompanied by direct amorphization. Neutron diffraction studies at IPNS identified structural instabilities which contributed to material failure. Highly accurate measurements of residual strains in ceramic composites are used to validate computer models for stress variation with temperature and the effects of interfacial fiber coatings on residual stress. Coarsening and lattice mis-match of γ' -type $\text{Ni}_3(\text{Al},\text{Si})$ particles in Ni-based alloys, which strongly influence coherency strains in these materials, are also measured directly using neutron scattering.

2. Time-of-flight neutron diffraction

Among the many areas of materials science where neutron diffraction has been effectively utilized, one of the most actively exploited is the measurement of elastic strains in industrially relevant materials. There are number of reasons for the popularity of these studies. Firstly, neutron beams interact very weakly with matter, giving rise to high penetration power. This means that strains calculated from neutron diffraction are representative of the bulk material, i.e., represent true engineering strains.

There are primarily two types of residual stress measurement. The first type measures macrostresses in single phase materials, as a function of position across an engineering component, using small volume (e.g., 1 x 1 mm) increments. These experiments are valuable for identifying regions of greatest strain, and thereby greatest weakness in materials such as aluminum and steel. The other type of experiment probes microstresses arising in multi-phase systems, where fabrication strains impact the mechanical behavior of the resulting industrial component. For interested readers, two recent review publications [1, 2] provide more detailed coverage of ongoing research in the field of residual stress determination with neutron diffraction.

When discussing diffraction measurements of residual stress, it is important to distinguish the two quantities stress and strain. Stress quantifies forces on a material due to outside influences. Strain is the measurable quantity which is the response of a material to stress. Residual strain is calculated as a fractional change in any crystallographic quantity which defines the fundamental spacings of atoms in a crystal. This is typically calculated using either the diffraction peak positions of selected reflections or an overall lattice parameter. Crystalline diffraction phenomena are measured based upon Bragg's Law:

$$\lambda = 2 d(hkl) \sin\Theta, \quad (1.1)$$

which relates the wavelength λ to interatomic plane spacings $d(hkl)$ and a scattering angle 2Θ . Most laboratory X-ray, and many neutron, diffractometers utilize a fixed wavelength source. A residual stress experiment, then, involves sampling an appropriate range of 2Θ to access the intensities and positions of desired reflections. At a pulsed neutron source, such as the Intense Pulsed Neutron Source (IPNS) at Argonne, a broad distribution of neutron wavelengths is produced via a process known

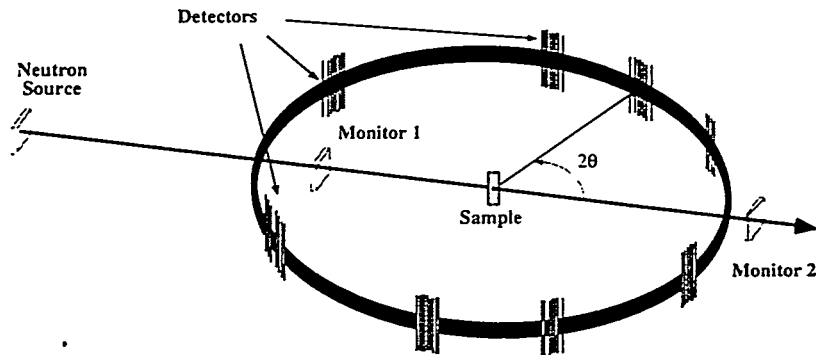


Figure 2.1 Schematic illustration of neutron powder diffraction layout of General Purpose Powder Diffractometer (GPPD) at IPNS. Scattering is in horizontal plane, with detectors positioned at fixed scattering angles.

as spallation, and diffraction patterns are accumulated at fixed scattering angles [1] (see Figure 2.1 for illustration).

Interpretation of time-of-flight (TOF) neutron diffraction patterns can be accomplished in many different ways. In regions where reflections are well isolated, peak positions, intensities and shape characteristics for individual reflections can be extracted. Alternatively, the entire diffraction pattern can be analyzed using the Rietveld profile refinement technique [4, 5] to extract overall lattice parameters. Using peak positions (d) or lattice parameters (a) from such analyses, compressive or tensile lattice strain can be calculated as

$$\varepsilon = \Delta d/d = (d - d_0) / d_0 \quad \text{or} \quad \varepsilon = \Delta a/a = (a - a_0) / a_0 \quad (1.2)$$

Fixed-angle TOF diffraction, as applied at IPNS, has a number of distinct advantages which have been exploited in the examples described below. Foremost among these is the ability to simultaneously measure strain in all phases in multi-phase composite materials and to directly quantify crystallographic and orientational anisotropies.

Highlighted in this paper are four recent examples of strain measurement in multi-component systems using neutron diffraction at the Intense Pulsed Neutron Source (IPNS) at Argonne National Laboratory (ANL). These illustrate the effects of: (i) chemical reaction between components, (ii) amorphization, (iii) fiber coatings, and (iv) coherent precipitation during coarsening.

3. Strain relaxation in WC-Co ceramic composites

WC-Co is a ceramic composite commonly used as a base material for cutting tools. During fabrication, however, thermal residual stresses (TRS's) are developed in the WC and Co as a result of differences in their coefficients of thermal expansion (CTE's). Co particles, randomly dispersed in WC, contract more on cooling, thereby generating a compressive strain on WC and experiencing tensile strain. At room temperature, these stresses are found to be isotropic (no variation with sample orientation). Monitoring of residual stresses at elevated temperatures is crucial to predicting the overall performance of this composite material.

Figure 3.1 shows the temperature dependence of residual strain for the a (basal plane) lattice parameter of WC, in a WC - 11 wt % Co composite (see Reference 6 for a complete report). In typical composite systems, strain decreases roughly linearly with temperature, converging to zero at the set-up temperature. These strain data are then used in computational models to predict mechanical properties at realistic operating temperatures. WC-Co, though, exhibits very unusual behavior at elevated temperatures. As seen in Fig. 3.1, the strain relaxation is distinctly non-linear, and exhibits dramatic hysteresis on cooling.

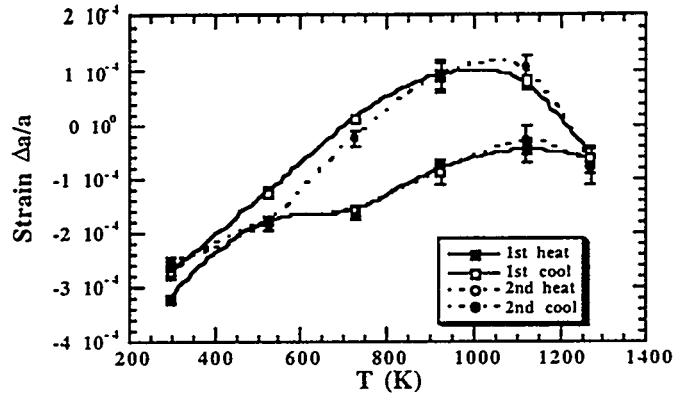


Figure 3.1 Residual strain in WC a (basal plane) lattice parameter in WC/Co composite as function of temperature. Solid curves are smooth fit to data for first heating and cooling cycle, while dashed curves are from second cycle. See text for details.

In fact, the complex strain variations closely follow changes in the mechanical properties of WC - 11 wt% Co, as determined by other methods. There are three distinct temperature domains, with differing mechanical and residual strain properties: (i) 300-900 K, where the composite is elastic and brittle, and the strain magnitude decreases (becomes less negative) steadily with increasing temperature, (ii) 900-1100 K, where the material is tough with limited plasticity, and the strain is reaching its minimum value, and (iii) above 1100 K, where there is extensive creep, and the strain shifts to higher magnitude. Subtle features in the strain plot can be explained by other known physical properties of this material. For instance, the change in slope at \sim 800-900 K corresponds with a maximum in the plot of internal friction with temperature. Furthermore, increasing strain above 1100 K is explained by chemical changes in the interaction interface; a portion of the WC is thought to react with Co to produce WCo_3 . Because WCo_3 has different elastic properties than Co, strains on WC from interaction with WCo_3 are changed. Finally, the hysteresis on cooling is thought to be related to differences in Co stacking fault reduction kinetics between heating and cooling. These results illustrate the tremendous power of neutron powder diffraction for quantifying mechanical effects which are only qualitatively understood by other analytical techniques.

4. Neutron irradiation of U_3Si

High density intermetallic alloys of uranium and silicon have been considered for use in high power-density nuclear applications and lower power-density, reduced enrichment applications. U_3Si and U_3Si_2 have received the most attention as reactor fuels. A fundamental stumbling block to their use in such applications, though, is the po-

tential for catastrophic swelling from plastic flow of amorphous material produced during irradiation.

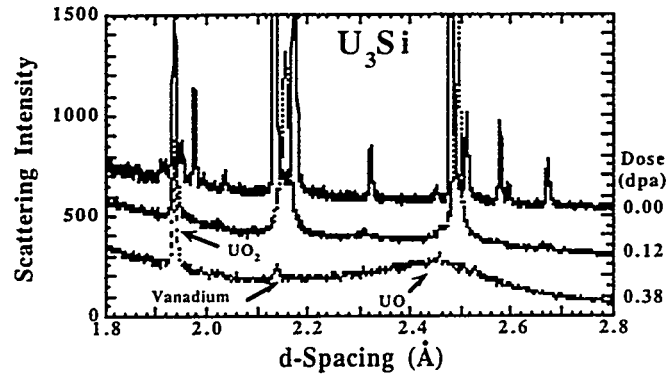


Figure 4.1 Diffraction data showing amorphization of U_3Si . Note that at 0.38 displacements per atom (dpa), the only remaining Bragg peaks are from uranium oxide impurities and from the vanadium sample container.

A study at IPNS, involving sequential neutron irradiation coupled with neutron powder diffraction analysis, identified structural changes induced by irradiation prior to complete amorphization. Given elsewhere are detailed reports for U_3Si [7] and U_3Si_2 [8]. Only results for U_3Si will be presented here. Neutron powder diffraction is an ideal probe for following changes resulting from neutron irradiation, because the high penetration of neutrons provides a bulk measurement. Un-irradiated

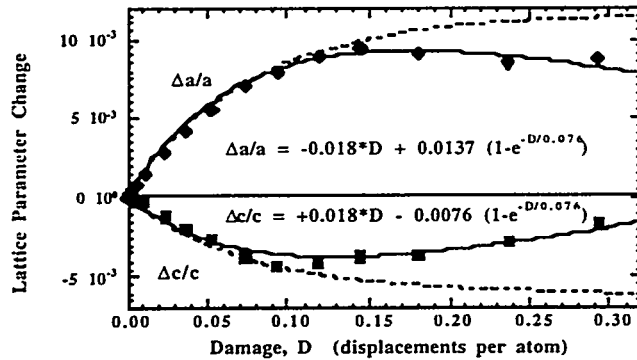


Figure 4.2 Strain in crystalline U_3Si as function of radiation damage. Initially, strain increases linearly with amorphous fraction (dashed curve). Beyond 0.10 dpa, strain is relieved as amorphous zones coalesce and migrate to surface.

U₃Si is fully crystalline with a tetragonal crystal structure closely related to cubic Cu₃Au. The degree of non-cubic character is defined by slight displacements of uranium atoms from idealized locations, and identified in the diffraction pattern by slight splitting of Bragg reflections. Neutron irradiation produces: (i) phase transformation to cubic, where U atoms move into a cubic arrangement and diffraction peaks merge in the diffraction pattern (see Fig. 4.1), (ii) direct amorphization of 100 Å zones (Fig. 4.1: amorphous scattering observed as broad undulations in the diffraction pattern), and (iii) lattice strain in the crystalline component (Fig. 4.2), due to a density mis-match between crystalline and amorphous zones.

Amorphous zones are produced in a sea of crystalline material, thus becoming *in situ* strain centers, and producing displacement fields projected onto the crystalline lattice. This produces a strain in the crystalline lattice to an extent determined by its elastic parameters and the relative volume fractions of crystalline and amorphous material. At low levels of damage, where the amorphous zones are isolated and buried in the interior of the macroscopic sample, residual strain on the crystalline lattice increases linearly with increasing amorphous fraction. At higher levels of damage, the zones begin to coalesce and migrate. Once a given zone reaches the surface, it no longer generates strain on the crystalline lattice, and the overall residual strain is reduced (see Fig. 4.2).

5. Strain mitigation in NiAl / Mo / Al₂O₃ coated-fiber composites

NiAl / Al₂O₃ metal matrix composites generally have very favorable mechanical properties for high temperature applications. Limitations are primarily associated with residual stresses in the NiAl matrix and Al₂O₃ fibers which produce matrix cracks via thermomechanical failure and ultimately degrade physical properties and service life. Thermal residual stresses are generated during fabrication due to a mismatch in the coefficients of thermal expansion (CTE's) of NiAl and Al₂O₃. Mitigation (reduction) of residual stresses, e.g. by coating the fibers, is critical for enhancing the thermomechanical durability of these composites.

A theoretical model [9] has been devised for predicting the effect of compliant and compensating fiber coatings as a function of coating thickness. Neutron diffraction experiments were performed [10] at IPNS to assess the influence of Mo coatings on Al₂O₃ fibers. Composites were prepared by consolidating coated fibers into NiAl by hot-isostatic pressing. Resulting samples contained 10-30 vol% parallel continuous Al₂O₃ fibers, fairly evenly distributed throughout the NiAl matrix. Diffraction experiments were carried out with the fibers horizontal and oriented 45° to the incident neutron beam. This facilitated simultaneous measurement of axial and transverse strains (see Fig. 2.1 for illustration). Strains were measured for 4 different Mo coating thicknesses: 0, 3, 10 and 30 μm.

Strains in NiAl were found to be tensile (>0) in the axial direction and generally compressive (<0) in the transverse direction (some values were extremely close

to zero). Figure 5.1 shows the variation of axial strain in NiAl as a function of coating thickness.

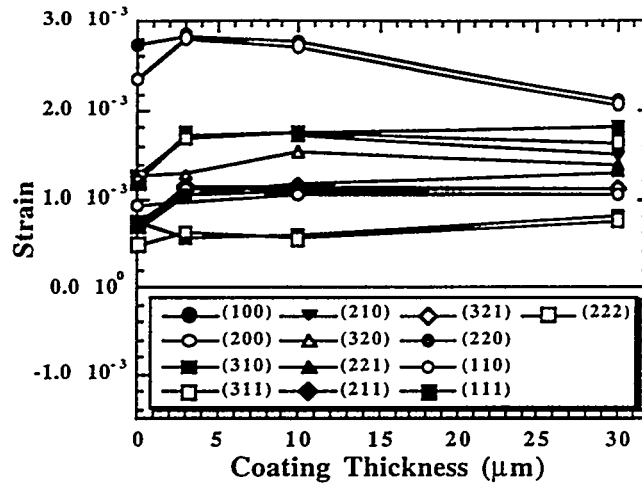


Figure 5.1 Axial strain in NiAl as function of Mo fiber-coating thickness. Each data point for given thickness represents different crystallographic orientation, as noted in the legend.

One of the unique characteristics of fixed angle time-of-flight neutron diffraction is the ability to obtain direct measurements of many types of anisotropy from a single diffraction run. For a highly anisotropic material, measurements in different detector banks quantify macroscopic anisotropy, i.e., tensile strain in the axial direction with compressive strain in the transverse. At the same time, measurements are made for all Bragg reflections, each of which represents a different orientation in the crystal. Strains in NiAl are orientationally anisotropic because the Al_2O_3 fibers are highly oriented. Anisotropy in the strain values for respective crystallographic directions is due to the high variability of the compliance factors in NiAl. These features are borne out in the strain measurements. There is a large spread in measured strain values, with those in the (100) direction for all coating thicknesses being 3-5 times those in the (111) direction. Data presented in Fig. 5.1 show a general trend to lower strain values with increasing coating thickness, in agreement with theory.

6. Lattice parameter changes in γ and γ' Ni-Al-Si during coarsening

Ternary Ni-based alloys, e.g., Ni-Al-Ti, Ni-Al-Mo and Ni-Al-Si, are often used as model systems for studying coarsening in multi-component systems. These alloys allow coherent precipitation of the ordered intermetallic $L1_2$ phase (Ni_3X , designated as γ') from a FCC-solid solution, and thus enable the study of coarsening of precipitates in coherent systems. With improvements in theoretical understanding of coars-

ening in multi-component systems, phase composition information (compositions of both precipitates and matrix) has become essential for proper interpretation of coarsening data obtained from ternary systems. Such information has not been readily available for most ternary systems, and prior to work at IPNS [11], non-existent for the Ni-Al-Si system.

γ' -L1₂-type intermetallic compounds of nominal composition Ni₃X are stable phases in the Ni-Al and Ni-Si binary systems, and in ternary Ni-Al-Si within a composition range described elsewhere [12, and references therein]. Also described in reference 11 are detailed studies of the effect of solute additions on the lattice parameters of γ -Ni solid solutions and Ni₃X compounds, which have provided analytical expressions relating composition to measured lattice parameter.

A neutron powder diffraction was undertaken at IPNS [11] to accurately measure lattice parameters for the γ and γ' type phases in a series of Ni-Al-Si samples, and to relate these results to coarsening data obtained from small angle neutron scattering. The diffraction pattern of γ' -Ni₃(Al,Si) is distinguishable from that of γ -Ni_x(Al,Si)_{1-x} by the introduction of new superlattice Bragg reflections due to crystallographic ordering of Ni and (Al,Si). Because the lattice parameters of the two phases are very close, the superlattice reflections are the only recognizable features from the γ' -phase (see Fig. 6.1). Furthermore, the additional reflections are comparatively weak, with intensities proportional to the difference in scattering amplitude

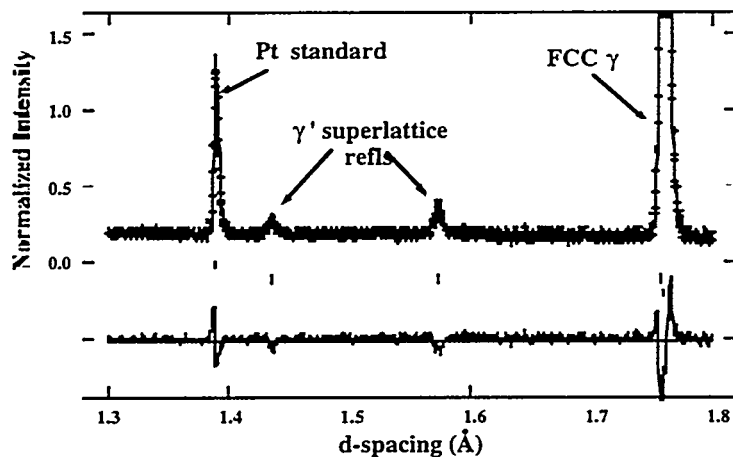


Figure 6.1 Small section of Rietveld profile refinement plot, showing modeling of Bragg scattering from Pt standard, γ -Ni₃(Al,Si), and γ' -Ni₃(Al,Si). "+" symbols represent observed data, smooth curve is calculated profile, and curve at bottom is difference between observed and calculated intensities. Tick marks identify Bragg peak positions.

between Ni and (Al,Si). Neutron diffraction was chosen over X-ray diffraction for this experiment because of the 60% improvement in sensitivity to this difference.

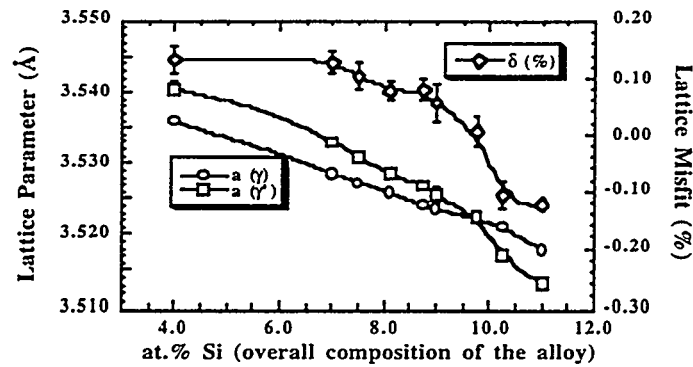


Fig. 6.2 Composition dependence of γ and γ' lattice parameters and of lattice mis-match parameter, $\delta = (a_{\gamma} - a_{\gamma'}) / a_{\gamma}$

All samples studied were prepared from $\text{Ni}_x(\text{Al,Si})_{1-x}$ alloys with x near 3.0, which were formed into buttons and aged at 600°C long enough to produce $\sim 600 \text{ \AA}$ particles. Rietveld profile refinements were carried out for each of the compositions. Pt foil was used as a standard for obtaining accurate calibration from one sample to the next. Lattice parameters for γ and γ' phases are given in Figure 6.2, along with the mis-match parameter, δ , calculated as the fractional difference between γ' and γ lattice parameters. γ' - $\text{Ni}_3(\text{Al,Si})$ is formed during aging via coherent precipitation from FCC $\text{Ni}_x(\text{Al,Si})_{1-x}$, meaning that γ' grains are directly correlated orientationally with their parent γ grains. This coherency can give rise to a strain between the two phases. Regions of greatest slope in the mis-match parameter curve (Fig. 6.2) correspond to compositions where coherency strains are most prevalent, and compositions unusual coarsening rates.

7. Concluding remarks

It is the author's hope that the foregoing examples have demonstrated the tremendous range of potential applications for time-of-flight neutron powder diffraction. In each of the cases described, highly precise structural parameters were obtained, which relate directly to the physical properties of the engineering materials in question. In many cases, however, the wealth of information present in the fine details is only fully understood when put in the context of other measurements. Certainly future work in this area will continue to rely heavily on complementary data; of particular value will be data derived from computer modeling, where experimental conditions can be simulated.

ACKNOWLEDGMENT

Work performed at Argonne National Laboratory is supported by the U.S. DOE-BES under contract No. W-31-109-ENG-38.

8. References

1. D.S. Kupperman (1994) Neutron-Diffraction Determination of Residual Stresses in Advanced Composites, *Annu. Rev. Mater. Sci.* **24**, 265-91.
2. M.T. Hutchings and A.D. Krawitz (1992) *Diffraction Measurement of Residual and Applied Stress Using Neutrons*, Kluwer Academic Publishers, Dordrecht.
3. J.D. Jorgensen, J. Faber, Jr., J.M. Carpenter, R.K. Crawford, J.R. Hauman, R.L. Hitterman, R. Kleb, G.E. Ostrowski, F.J. Rotella and T.G. Worlton (1989) Electronically Focused Time-of-Flight Powder Diffractometers at the Intense Pulsed Neutron Source, *J. Appl. Cryst.* **21**, 321.
4. H.M. Rietveld (1969) A Profile Refinement Method for Nuclear and Magnetic Structures, *J. Appl. Cryst.* **2**, 65.
5. A.C. Larson and R.B. Von Dreele (1986) GSAS, General Structure Analysis System. Los Alamos National Laboratory Report LAUR86-748.
6. D. Mari, A.D. Krawitz, J.W. Richardson, Jr. and W. Benoit (1996) Residual Stress in WC-Co Measured by Neutron Diffraction *Mater. Sci. Eng. A*, **A209**, 197-205.
7. R.C. Birtcher, J.W. Richardson, Jr. and M.H. Mueller (1997) Amorphization of U_3Si by Ion or Neutron Irradiation, *J. Nucl. Mat.* **244**, 251-7.
8. R.C. Birtcher, J.W. Richardson, Jr. and M.H. Mueller (1996) Amorphization of U_3Si_2 by Ion or Neutron Irradiation, *J. Nucl. Mat.* **230**, 158-63.
9. S.M. Arnold, V.K. Arya and M.E. Melis (1992) Reduction of Thermal Residual Stresses in Advanced Metallic Composites Based upon a Compensation/Compliant Layer Concept, *J. Composite Mater.*, **26** (9), 1287-1309.
10. D.E. Boss (1997) The Effect of Fiber Coatings on the Residual Stresses in Sapphire / NiAl Composites, PhD dissertation, Northwestern University.
11. G. Muralidharan, J.W. Richardson, Jr., J.E. Epperson and H. Chen (1997) Lattice Parameters and Composition of γ and γ' During Coarsening in the Ni-Al-Si System: A Neutron Powder Diffraction Study, *Scripta Mater.*, **36** (5), 543-9.
12. G. Muralidharan, J.E. Epperson and H. Chen (1996) Experimental Studies on the Effect of Coherency Strains on Coarsening Kinetics: Current Status and Future Outlook, in *Advances in Physical Metallurgy*, Eds. S. Banerjee and R.V. Ramanujan, Gordon and Breach Publishers, New York, 333.